ZOOLOGICAL RESEARCH

Magnetic brain stimulation using iron oxide nanoparticle-mediated selective treatment of the left prelimbic cortex as a novel strategy to rapidly improve depressive-like symptoms in mice

Qing-Bo Lu[1,#], Jian-Fei Sun[2,#,*], Qu-Yang Yang[2], Wen-Wen Cai[1], Meng-Qin Xia[1], Fang-Fang Wu[1], Ning Gu[2,*], Zhi-Jun Zhang[1,*]

[1] *Department of Neurology*, *Affiliated Zhongda Hospital*, *School of Medicine*, *Institution of Neuropsychiatry*, *Southeast University*, *Nanjing*, *Jiangsu* 210009, *China*

[2] *State Key Laboratory of Bioelectronics*, *Jiangsu Key Laboratory of Biomaterials and Devices*, *School of Biological Science and Medical Engineering*, *Southeast University*, *Nanjing*, *Jiangsu* 210009, *China*

ABSTRACT

Magnetic brain stimulation has greatly contributed to the advancement of neuroscience. However, challenges remain in the power of penetration and precision of magnetic stimulation, especially in small animals. Here, a novel combined magnetic stimulation system (c-MSS) was established for brain stimulation in mice. The c-MSS uses a mild magnetic pulse sequence and injection of superparamagnetic iron oxide (SPIO) nanodrugs to elevate local cortical susceptibility. After imaging of the SPIO nanoparticles in the left prelimbic (PrL) cortex in mice, we determined their safety and physical characteristics. Depressive-like behavior was established in mice using a chronic unpredictable mild stress (CUMS) model. SPIO nanodrugs were then delivered precisely to the left PrL cortex using *in situ* injection. A 0.1 T magnetic field (adjustable frequency) was used for magnetic stimulation (5 min/session, two sessions daily). Biomarkers representing therapeutic effects were measured before and after c-MSS intervention. Results showed that c-MSS rapidly improved depressive-like symptoms in CUMS mice after stimulation with a 10 Hz field for 5 d, combined with increased brain-derived neurotrophic factor (BDNF) and inactivation of hypothalamic-pituitary-adrenal (HPA) axis function, which enhanced neuronal activity due to SPIO nanoparticle-mediated effects. The c-MSS was safe and effective, representing a novel approach in the selective stimulation of arbitrary cortical targets in small animals, playing a bioelectric role in neural circuit regulation, including antidepressant effects in CUMS mice. This expands the potential applications of magnetic stimulation and progresses brain research towards clinical application.

Received: 25 April 2020; Accepted: 12 May 2020; Online: 13 May 2020

Foundation items: This work was supported by grants from National Natural Science Foundation of China (81830040 to Z.J.Z.), National Key Projects for Research and Development Program of China (2016YFC1306700 to Z.J.Z., 2017YFA0104302 to N.G., and 2017YFA0104301 to J.F.S.), and Program of Excellent Talents in Medical Science of Jiangsu Province (JCRCA2016006 to Z.J.Z.)

[#]Authors contributed equally to this work

*Corresponding authors, E-mail: sunzaghi@seu.edu.cn; guning@seu.edu.cn; janemengzhang@vip.163.com

DOI: 10.24272/j.issn.2095-8137.2020.076

Keywords: SPIO nanoparticles; Magnetic stimulation; Bioelectronics; Depression

INTRODUCTION

Physical therapies have been increasingly used for the prevention and treatment of a wide range of diseases in humans (Diana et al., 2017; Polanía et al., 2018). For example, repetitive transcranial magnetic stimulation (rTMS) has been used to treat neuropsychiatric disorders due to its non-invasive, convenient, and effective properties (Hauer et al., 2019; Trevizol & Blumberger, 2019). However, there remain technical limitations to rTMS, including poor penetrating power, lack of precision in magnetic stimulation, limited depth of stimulation, and inadequate ability to focus on target brain regions. In particular, in small animals such as rats and mice (Fang & Wang, 2018; Sun et al., 2011), even the smallest universal coil will stimulate a whole hemisphere or even the complete brain (Salvador & Miranda, 2009; Tang et al., 2016). It is therefore a challenge to accurately identify the underlying molecular and neural circuit mechanisms within target regions (Guadagnin et al., 2016; Meng et al., 2018). Thus, there is a need to improve technology to satisfy the rapid development of brain science research.

Non-selectivity could be attributed to the low susceptibility χ of biological tissues. There are various effects that result from magnetic fields, including direct magnetization and indirect magneto-electrical, magneto-elastic, or magneto-thermal effects. However, the consequences of these effects rely on the susceptibility of tissues. Regarding brain stimulation, magneto-electric induction is a common neural regulatory principle (Bestmann, 2008; Tarapore et al., 2016). Magneto-electric induction can be expressed using Faraday's law:

$$\nabla \times \vec{E} = -\frac{\partial \vec{B}}{\partial t} = -\frac{\partial(\mu \vec{H})}{\partial t} \quad (1)$$

where t is time, $\vec{E}$ is the induction electric field, $\vec{B}$ is the magnetic flux density, $\vec{H}$ is the magnetic field intensity, and μ is the local tissue permeability. Given that permeability μ is very small, field intensity $\vec{H}$ must be very high to yield an adequately strong electric field. Similarly, the region of focus cannot be too small. As an alternative, augmentation of μ can essentially alter the level of magnetic stimulation and overcome the current drawbacks of this technique. Given the remarkable development of nanotechnology, superparamagnetic iron oxide (SPIO) nanoparticles, which exhibit excellent biocompatibility, offer a great opportunity to advance research (Li et al., 2017). Targeted delivery of SPIO nanoparticles into a specific tissue could significantly enhance the local susceptibility of tissues. When a weak magnetic field covers multiple cortical areas, only the region containing SPIO nanoparticles would be activated, with little influence elsewhere. This technique would allow the magnetic effect, rather than the magnetic field, to be focused on a specific tissue for precise stimulation. Theoretically, this strategy could stimulate nearly any tissue that contains SPIO nanoparticles. We have termed this stimulation technique a combined magnetic stimulation system (c-MSS).

Application of magnetic nanomaterials in neuroscience has attracted increasing interest from researchers, with several excellent reports on neural regulation based on targeted binding of magnetic nanoparticles and neurons (Chen et al., 2015; Huang et al., 2010; Roet et al., 2019). By activation of ion channels with the magneto-thermal effect, neural function can be controlled. In addition to the magneto-thermal effect, the influence of magneto-electric nanoparticles upon intrinsic neuro-electric signals has been predicted and studied (Guduru et al., 2015; Yue et al., 2012). However, reports on the successful application of nanoparticle-dependent magnetic stimulation in neurological disorders remain scarce. Here, for the first time, we tested the action of c-MSS in a depressive-like animal model. Our results showed that the magnetic effect of magnetic iron oxide nanoparticles on the cortex significantly improved neurological symptoms.

Major depressive disorder (MDD) is a common and severe mental disorder in humans (Otte et al., 2016), causing the highest disability-adjusted life years (DALYs) and total disease burden of all mental diseases (GBD 2016 Disease and Injury Incidence and Prevalence Collaborators., 2017). Transcranial magnetic stimulation (TMS) was first used as an anti-depressive therapy in 1996, with high-frequency (10 Hz) magnetic field targeting of the left dorsolateral prefrontal cortex (DLPFC) for clinical intervention in treatment-resistant depression (TRD) approved in 2008 by the US Food and Drug Administration (US-FDA) (Pascual-Leone et al., 1996). In the present study, we explored whether depressive-like behavior in mice could be quickly and effectively improved by c-MSS stimulation of the left prelimbic (PrL) cortex, considered to be potentially homologous to the DLPFC in primates (Vertes, 2006). Because of its mild field and precise action, this technique could greatly expand the applicability of magnetic stimulation in anti-depression. Moreover, *in vivo* magnetic resonance imaging (MRI) demonstrated that the magnetic nanoparticles were stably retained within the PrL cortex during the treatment period. Furthermore, SPIO nanoparticle toxicity and safety were investigated in cultured primary cortical neurons and in brain tissue of mice. The antidepressant effects in chronic unpredictable mild stress (CUMS) mice were also investigated preliminarily. Importantly, field frequency and treatment duration were determined for optimization of treatment effects. This novel approach should complement clinical rTMS, playing an important role in neuroscience research with small animals.

MATERIALS AND METHODS

Establishment of c-MSS

The c-MSS consisted of SPIO nanodrugs and a magnetic pulse sequence. The SPIO nanodrugs were polyglucose sorbitol carboxymethylether (PSC)-coated γ-Fe_2O_3 nanoparticles (trade name: Ferumoxytol), manufactured by the

Zhengda Tianqing Pharmaceutical Enterprise (China) and approved by the Chinese FDA for clinical use.

The magnetic pulse sequence was generated by the rotation of a pair of tapered magnets (NdFeB permanent magnet, N45, Innuovo, China) symmetrically attached to a motor (IKA RW20 Digital, Germany) using a rigid plastic crossbar. Rotational speed of the motor could be adjusted continuously. The heads of the experimental mice were placed within the magnetic field. For mice, the wave profile was a pulse sequence. A rotational speed of 300 r/min corresponded to a frequency of 10 Hz because the pair of magnets yielded two pulses every cycle. Magnetic flux density was measured using a gauss meter (HT20, Hengtong, China). During all experiments, the apparatus was maintained in a humidity- and temperature-controlled environment.

Observation of SPIO nanoparticles by MRI

The procedure for SPIO nanodrug injection into the left PrL cortex of mice is presented in Supplementary Note S1. The MRI (Bruker BioSpec Horizontal 7.0 T) scans were then performed on days 1, 3, 5, 7, and 11 after stereotactic microinjection of the SPIO drugs for *in vivo* imaging of the PrL cortex. Details on the MRI procedure are described in Supplementary Note S2.

Safety evaluation of SPIO nanoparticles in cultured neurons and brain tissue of mice

Cell counting kit-8 (CCK-8) assay: Viability of primary cortical neurons (details shown in Supplementary Note S3) was measured over time using a CCK-8 kit (Dojindo, Kumamoto, Japan). Primary cortical neurons were incubated with 5 μg/mL SPIO nanodrugs to measure dependency of cytotoxicity with time (0, 6, 12, 24, and 48 h) and nanodrug concentration (0, 5, 25, 125, and 625 μg/mL) over 24 h. Calculation of cellular viability is detailed in Supplementary Note S4.

Lactate dehydrogenase (LDH) release analysis: Experimental design was identical to that of the CCK-8 assay. LDH release into culture supernatants was measured using an LDH cytotoxicity assay kit (Beyotime Co., Shanghai, China). Maximal LDH release was determined in primary cortical neurons lysed by incubation in lysis buffer at room temperature for 60 min. Mean LDH release of control neurons was indexed to 100%, the value used for normalization.

Terminal deoxynucleotidyl transferase-mediated deoxyuridine triphosphate nick end-labeling (TUNEL) assay for apoptosis: A TUNEL kit (Invitrogen, Carlsbad, CA, USA) was used for evaluating apoptosis in the left PrL cortex of experimental mice. The tissue was sliced after 5 days of treatment by c-MSS. The rate of apoptosis was determined by enumerating TUNEL-positive cells in six random fields in the left PrL cortex in comparison with total number of cells using ImageJ software.

Preliminary analysis of physical mechanism of c-MSS

The physical effects of c-MSS were assessed in a hydrogel phantom, in which SPIO nanoparticles were injected into a model of tissue. The amount of SPIO nanoparticles was the same as that injected *in vivo* (1.67 mg/mL, 300 nL). The fabrication process is presented in Supplementary Note S5.

Measurement of magnetic heating effect: A fiber sensor (FISO UMI 8, Canada, measuring range: –4 ℃–100 ℃) was inserted into the cubic hydrogel, with its tip inside the SPIO nanoparticles. The temperature sensor was connected to a workstation to record data. The induction current curve was plotted using Origin software.

Measurement of magneto-acoustic signals: The magneto-vibration effect of SPIO nanoparticles within a 10 Hz magnetic field was measured using acoustic signals. The hydrogel phantom and acoustic transducer were submerged in deionized water at a distance of 45 mm. Acoustic signals were recorded using a transducer (S/N 240992 , Olympus Ltd., Japan), and then amplified (5058PR, Olympus Ltd., Japan). Finally, the signals were digitized and displayed on an oscilloscope (DSOX4054A, Keysight Technologies, USA).

Measurement of magnetic field induction voltage: The magnetic field generator and hydrogel phantom were placed inside a Faraday cage to eliminate external electrical noise. A glass microelectrode containing artificial cerebrospinal fluid (126 mmol/L NaCl, 3 mmol/L KCl, 24 mmol/L $NaHCO_3$, 1.25 mmol/L NaH_2PO_4, 2 mmol/L $CaCl_2$, 2 mmol/L $MgSO_4$, and 10 mmol/L glucose; resistance: 2–5 MΩ) was used to record local field potential in the hydrogel phantom. An Ag/AgCl wire was used as a reference electrode. The field potential was amplified (Axoprobe 1A, Axon Instruments, USA), filtered using a band-pass filter (Neurolog NL125, Digitimer Ltd., UK) to exclude signals outside the 2 to 200 Hz range, then digitized using an analog-to-digital conversion (ADC) board (CED 1401 plus, Cambridge Electronic Design, UK) and recorded using Spike 2 software (Cambridge Electronic Design, UK).

Establishing, evaluating, and screening depressive-like mouse model

Experimental animals: All experiments were performed on male C57BL/6 JAX^{TM} mice (age: 6–8 weeks; weight: 18–24 g, Sino-British SIPPR/BK Lab Animal Ltd., China). Details of animal husbandry are described in Supplementary Note S6. All animal experiments were conducted strictly in accordance with the National Institutes of Health Guide for the Care and Use of Laboratory Animals and approved by the Animal Study Committee of Southeast University, China (permit No. 20180501006).

Establishing chronic unpredictable mild stress model and confirming sensitive depressive-like symptoms: Behavioral tests, including a sucrose preference test (SPT) and forced swim test (FST), were used to evaluate, screen, and identify sensitive depressive-like mice as the initial stage of the CUMS mouse model. The behavioral tests are described in Supplementary Note S7 and the detailed modelling process is described in Supplementary Note S8.

Selecting and optimizing therapeutic schedule for CUMS mice using c-MSS

Selection of optimized frequency: A total of 0.5 μg of SPIO

nanoparticles (1.67 mg/mL, 300 nL) were microinjected into the left PrL cortex of each CUMS mouse. During the c-MSS treatment, all experimental mice were placed in an aluminum restraint while awake. Mice were allocated into four groups: without magnetic field intervention or treated by c-MSS (2, 5, or 10 Hz) twice daily (5 min duration each time, once in the morning and once in the afternoon) for 5 days.

Selection of optimized duration of treatment: After selection of optimized frequency, as described above, the same volume of SPIO nanoparticles was microinjected into the left PrL cortex of fresh CUMS mice. Depending on group allocation, the mice were treated in a 10 Hz magnetic field for 1, 3, 5, or 7 days.

Confirmation of anti-depressive effectiveness of c-MSS: The effectiveness of c-MSS was evaluated by comparing the treated CUMS mice with control animals. The CUMS mice were allocated into four groups, those injected with saline and treated with 10 Hz magnetic field stimulation (CUMS+Saline+10 Hz MF), those injected with Au nanoparticles and treated with 10 Hz magnetic field stimulation (CUMS+Au+10 Hz MF), those injected with SPIO nanoparticles but without magnetic field stimulation (CUMS+SPIO), and those injected with SPIO nanoparticles and treated with 10 Hz magnetic field stimulation (CUMS+10 Hz c-MSS). The frequency and duration of the magnetic stimulation treatment was consistent with that described above (10 Hz for 5 days). Treatment effectiveness was evaluated using SPT and FST.

Measurement of biomarkers of effective treatment of depression

Animal sacrifice and sample preparation: All procedures related to animal sacrifice and preparation are detailed in Supplementary Note S9.

c-fos testing by immunohistochemistry: The expression of c-fos protein was measured using standard immunohistochemistry protocols. Details on the procedure are described in Supplementary Note S10.

Testing of brain-derived neurotrophic factor (BDNF) by immunoblot analysis: The complete left PrL cortex tissue was analyzed for the expression of BDNF protein. The detailed procedure is described in Supplementary Note S11.

Testing of adrenocorticotropic hormone (ACTH) and corticosterone (CORT) levels in serum: The concentrations of ACTH and CORT were determined using an enzyme-linked immunosorbent assay (ELISA) (Angel Gene, China) as a measure of the hyperactivation of the hypothalamic-pituitary-adrenal (HPA) axis, in accordance with the manufacturer's protocols.

Statistical analysis

Statistical analyses were conducted using GraphPad Prism 7 (GraphPad Software Inc., USA). Results are expressed as mean±*SEM*. Multiple-group comparisons were achieved using one-way analysis of variance (ANOVA) followed by Bonferroni's *post hoc* test.

RESULTS

Establishment of c-MSS

The mean core diameter and entire structure of the γ-Fe_2O_3 nanoparticles were approximately 9 nm and 30 nm, respectively (Figure 1A, C). The inset in Figure 1A shows an external view of the nanodrugs and a schematic of the nanodrug injections (300 nL, 1.67 mg/mL) into the left PrL cortex of experimental mice in Figure 1B. Generation of the magnetic field is shown in Figure 1D. Magnetic flux was simulated using Ansoft software (Figure 1E). The nanoparticles were superparamagnetic and uniformly dispersed without significant aggregation (Figure 1F). The actual output wave profile is shown in Figure 1G, which was a continuous pulse sequence with a half width of ~30 μs. The cone shape of the magnets was to reduce pulse width. Peak field intensity in the brains of mice was 100 mT. Frequency was tuned by adjusting the rate of rotation. We hypothesized that the left PrL cortex would be stimulated magnetically every time the magnet passed over the mouse brain.

Imaging of SPIO nanoparticles by MRI

After microinjection into the left PrL cortex of CUMS mice, the SPIO nanoparticles were imaged *in vivo* using MRI. The injected SPIO nanoparticles were visible as sphere-like dark regions by MRI and remained stable and aggregated within the left PrL cortex for at least 11 days (Figure 2A–D).

Safety evaluation of SPIO nanoparticles in cultured neurons and brains of mice

A SPIO nanodrug suspension (100 μL) was placed in a 96-well plate in which primary neurons were growing for evaluation of cell viability. In the animal experiments, the SPIO nanoparticles were injected into the left PrL cortex of mice at a volume of 0.5 μg. A corresponding concentration of 5 μg/ml was used for 100 μL of culture medium, and the *in vitro* safety of the SPIO nanodrugs was evaluated at concentrations of 5 μg/mL to 625 μg/mL. After 24 h of co-culture, significant cytotoxicity occurred only at the highest concentration of 625 μg/mL (P<0.01, Figure 2E, F). Experiments investigating the time dependency of cytotoxicity demonstrated that 5 μg/ml SPIO nanoparticles over the study time range were not toxic (Figure 2G, H). TUNEL assay demonstrated that left PrL cortical slices treated by microinjection of SPIO nanodrugs showed a non-significant increase in cell apoptosis in the four mouse groups compared with that observed in the control mice after 5 days (Figure 2I, J).

Preliminary analysis of physical mechanism of c-MSS in hydrogel phantom

Firstly, the SPIO nanoparticles did not cause significant heating in the hydrogel phantom when placed within a 10 Hz magnetic field (Figure 3A). Heating curves demonstrated only a small temperature rise over a 1 h period (Figure 3B). Secondly, no acoustic signal was identified within the 5, 10, or 15 Hz magnetic fields of the phantom, thus, any magneto-vibration effect of the SPIO nanoparticles could be ignored

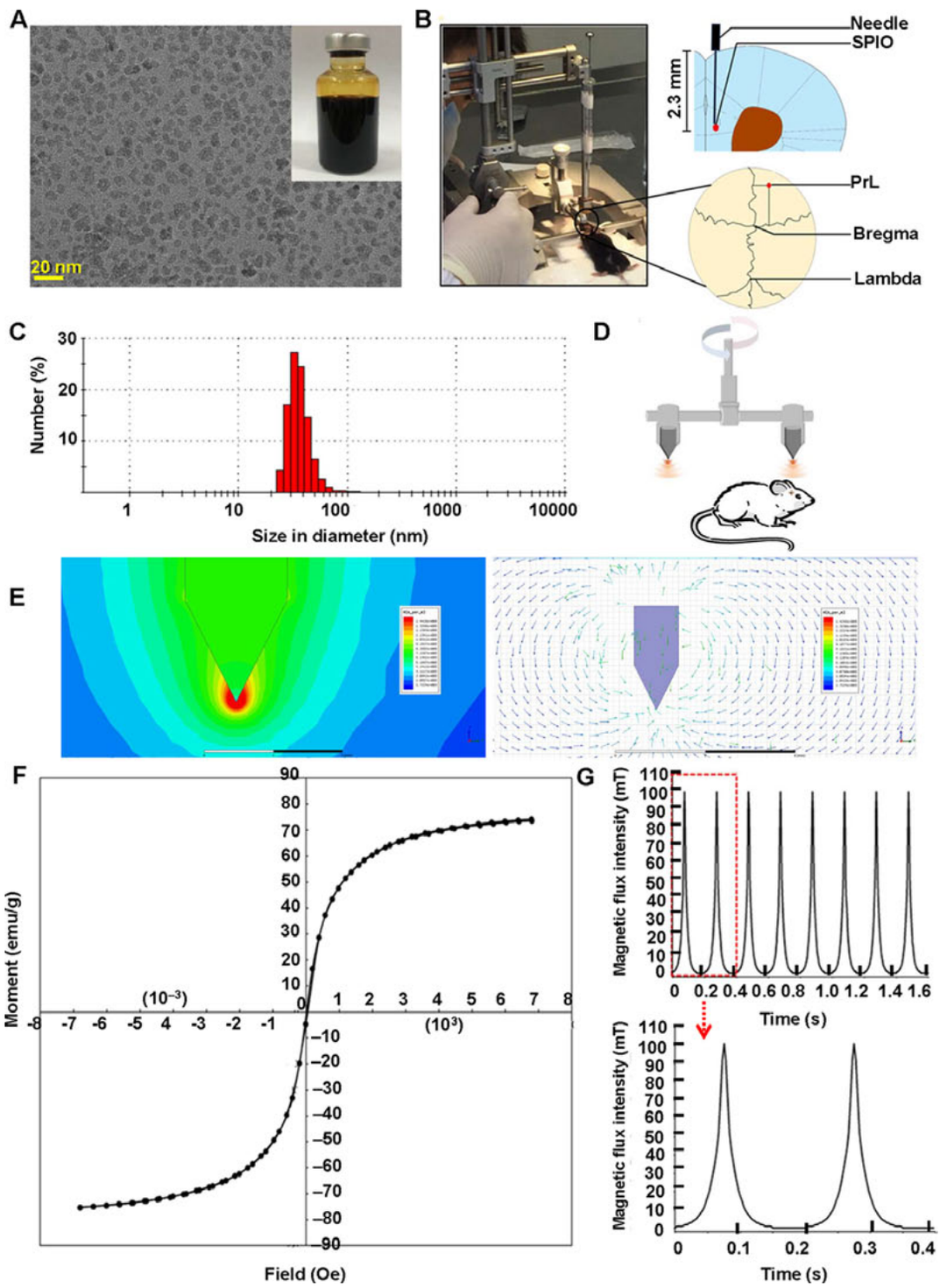

Figure 1 Construction of combined magnetic stimulation system (c-MSS) and microinjection of mice

A: TEM image of PSC-capped γ-Fe_2O_3 nanoparticles and external view of injection (Inset). B: Schematic of injection process in left PrL cortex of mice. C: Measurement of PSC-capped γ-Fe_2O_3 nanoparticle size using Dynamic Light Scattering. Mean diameter was approximately 30-35 nm. D: Schematic of imposed magnetic field. E: Simulation of field intensity and magnetic flux of cone-shaped magnets. F: Magnetic hysteresis of SPIO nanoparticles. G: Output wave-profile of magnetic field. c-MSS: Combined magnetic stimulation system; TEM: Transmission electronic microscopy; PSC: Polyglucose sorbitol carboxymethylether; PrL: Prelimbic; SPIO: Superparamagnetic iron oxide.

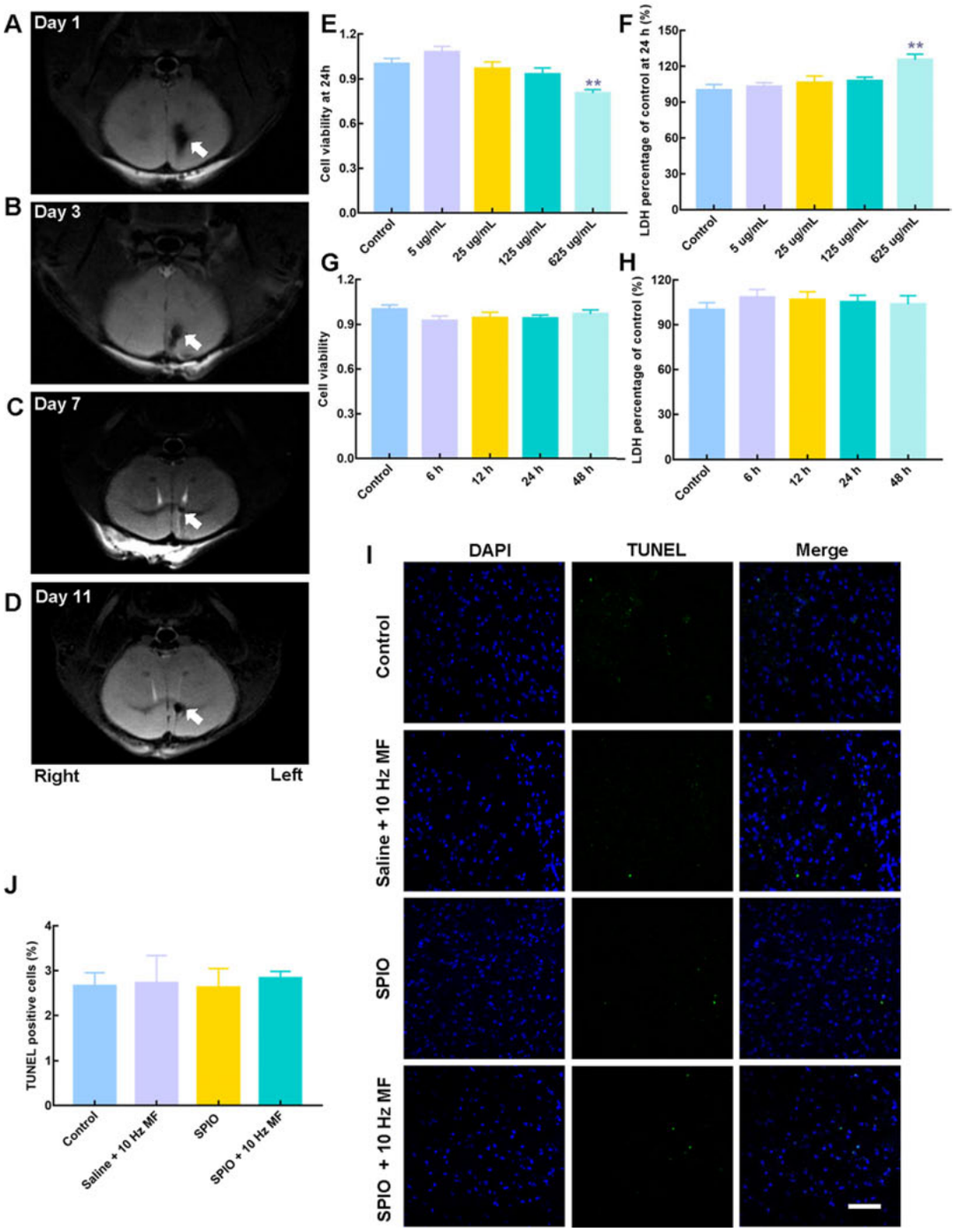

Figure 2 MRI tracing and cytotoxicity of nanodrugs

A–D: *in vivo* MRI images of injected nanodrugs in left PrL cortex of mice after 1, 3, 7, and 11 days, respectively. n=3 in each group. E, F: CCK-8 and LDH assay of primary cortical neurons after treatment for 24 h with various doses of SPIO nanoparticles. G, H: CCK-8 and LDH assay of primary cortical neurons treated with 5 μg/mL SPIO nanoparticles for 6, 12, 24, and 48 h (n=8). I: Representative images of *in situ* TUNEL assay using confocal microscopy (magnification,×400). J: Percentage of TUNEL-positive cells. Scale bar: 50 μm. n=8 slices from eight mice in each group. **: P<0.01 compared with control group (one-way ANOVA followed by Bonferroni's multiple comparison *post hoc* test). MRI: Magnetic resonance imaging; PrL: Prelimbic; CCK-8: Cell counting kit-8; LDH: Lactate dehydrogenase; SPIO: Superparamagnetic iron oxide; TUNEL: Terminal deoxynucleotidyl transferase-mediated deoxyuridine triphosphate nick end-labeling.

(Figure 3C). Thirdly, a magneto-electric induction effect was observed in the phantom using an electrophysiological recording system, with decreased induction voltage as field frequency increased in the absence of SPIO nanoparticles, indicating that high frequency caused the pulse sequence to resemble a direct-current field (Figure 3D, E). Interestingly, the induction voltage within the 10 Hz magnetic field was significantly enhanced when the SPIO nanoparticles were present (Figure 3F). The physical effects of the c-MSS were also simulated using COMSOL software. It was found that the SPIO nanoparticles enhanced the magnetization, magneto-vibration, and magneto-electrical induction effects under pulse

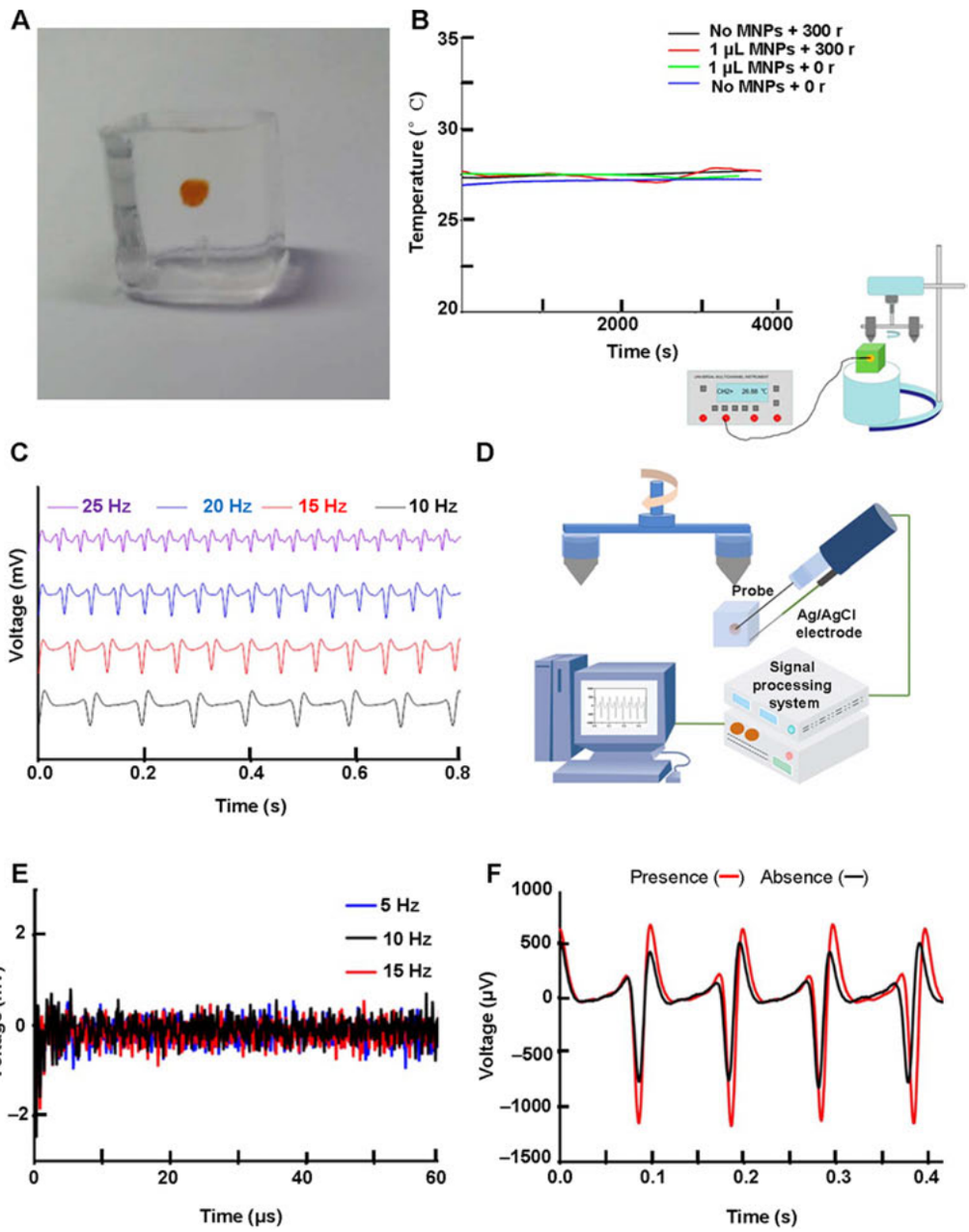

Figure 3 Measurement of magneto-electric induction and physical effects in a hydrogel phantom

A: Hydrogel phantom containing injected SPIO nanoparticles. B: Heating of phantom within a 10 Hz (300 r/min) magnetic field. C: Magneto-electric induction in different field frequencies. D: Schematic of measurement of magneto-electric induction. E: Acoustic signals of phantoms with SPIO nanoparticles in presence of a 5, 10, and 15 Hz magnetic field. F: Induced voltages in presence or absence of SPIO nanoparticles. Result was confirmed in triplicate. SPIO: Superparamagnetic iron oxide.

sequences of the magnetic field in tissue. More importantly, these effects were highly restricted to regions around the SPIO nanoparticle surfaces (Figure 4).

Establishing, evaluating, and screening depressive-like mice

The experimental procedure is shown in Figure 5A. After the

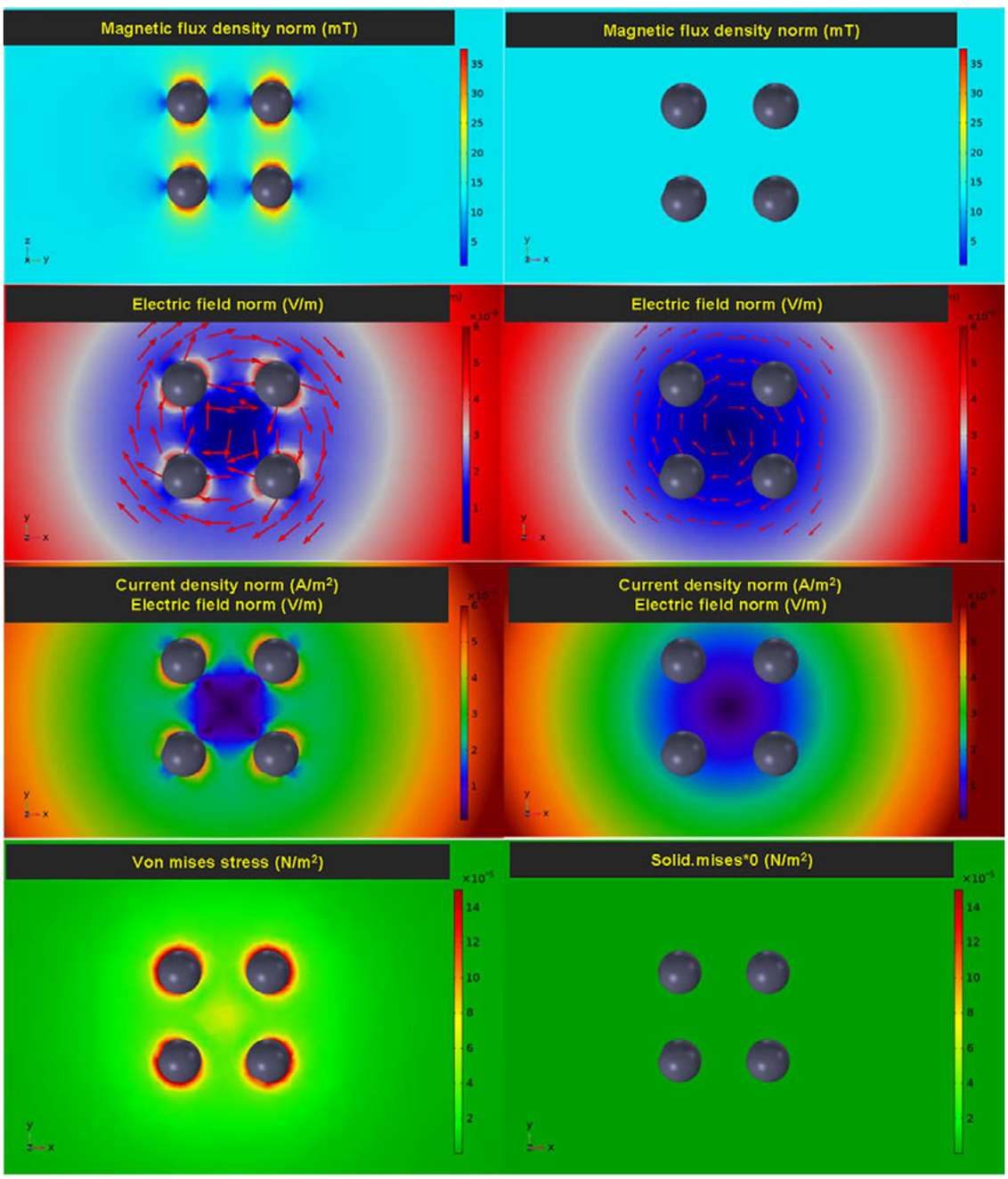

Figure 4 Simulation using COMSOL software of magnetization, induction of electric field, induction of electric current, and induction of stress field for SPIO nanoparticles in presence of a 10 Hz magnetic field

Left column represents magnetic spheres; right column represents non-magnetic spheres.

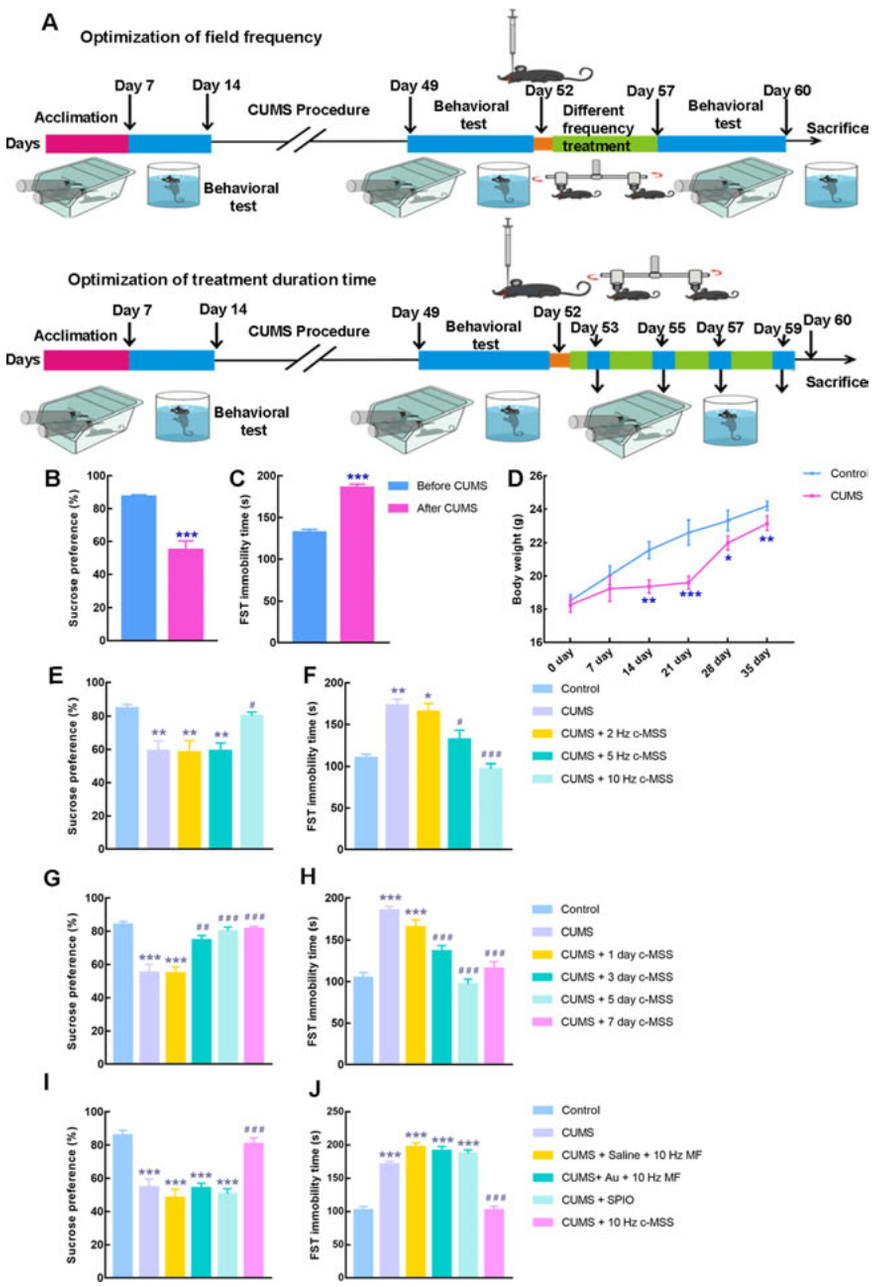

Figure 5 Treatment of CUMS mice and confirmation of effects of c-MSS through behavioral experiments

A: Experimental procedures for selection of optimal field frequency and duration of treatment. B, C: SPT and FST results in CUMS mice. *n*=15 mice for each group. Values are mean±*SEM*. ***: $P<0.001$ vs. before CUMS modelling (control mice) (paired Student's *t*-test). D: Monitoring of body weight of mice compared with age-matched control mice. *n*=15 mice for each group. Values are mean±*SEM*. *: $P<0.05$ vs. Control; **: $P<0.01$ vs. Control; ***: $P<0.001$ vs. Control. E, F: SPT and FST results in CUMS mice after c-MSS treatment using different frequencies of magnetic field. G, H: SPT and FST results in CUMS mice after treatment with a 10 Hz c-MSS for a variety of durations. Values are mean±*SEM*, *n*=8-10 mice. *: $P<0.05$ vs. Control; **: $P<0.01$ vs. Control; ***: $P<0.001$ vs. Control. #: $P<0.05$ vs. CUMS; ##: $P<0.01$ vs. CUMS; ###: $P<0.001$ vs. CUMS (one-way ANOVA followed by Bonferroni's multiple comparison *post hoc* test). I,J: SPT and FST results. Sham groups were administered saline and 10 Hz magnetic field, SPIO nanoparticles without a magnetic field, and Au nanoparticles in a 10 Hz magnetic field. All treatments lasted 5 days (two 5 min sessions per day). Data were calculated from six mice for each group. Values are mean±*SEM*. ***: $P<0.001$ vs. Control. ###: $P<0.001$ vs. CUMS (one-way ANOVA followed by Bonferroni's multiple comparison *post hoc* test). c-MSS: Combined magnetic stimulation system; FST: Forced swim test; SPT: Sucrose preference test; CUMS: Chronic unpredictable mild stress; SPIO: Superparamagnetic iron oxide; PrL: Prelimbic.

CUMS procedure, 65% of mice exhibited depressive-like symptoms and were subsequently utilized in follow-up studies, as confirmed by significantly reduced sucrose consumption in the SPT (Figure 5B) and increased immobility time in the FST (Figure 5C). Furthermore, the successful establishment of CUMS mice was partly confirmed by the significant decrease in body weight during weeks 2–5 compared to the age-matched control mice (Figure 5D).

Selection and optimization of therapeutic schedule for CUMS mice by c-MSS

Firstly, the frequency optimization tests indicated that only stimulation with 10 Hz c-MSS for 5 days significantly improved depressive-like behavior in CUMS mice, as indicated by increased sucrose consumption in the SPT and reduced immobility time in the FST (Figure 5E, F). Consequently, a 10 Hz magnetic stimulation regimen was used in subsequent experiments. Secondly, improvement in depressive-like behavior was observed after 3 days of treatment, which became prominent and stable after 5 days of treatment using the c-MSS (Figure 5G, H).

To further confirm the specific therapeutic effects of SPIO nanoparticles on CUMS mice, Au nanoparticles were microinjected into their left PrL cortices under c-MSS conditions. As expected, experimental mice, in which the anti-depressive effects of c-MSS were confirmed, exhibited significantly increased sucrose consumption in the SPT and decreased immobility time in the FST in the 10 Hz c-MSS group compared with the other four groups (Figure 5I, J). The Au nanoparticles showed identical morphology and size as the SPIO nanoparticles but did not improve the behavior of mice. Taken together, these findings indicate that the observed anti-depressive effects resulting from enhanced magnetic stimulation were due to the use of SPIO nanoparticles.

Testing of biomarkers for effective anti-depression in mice

Firstly, expression of the c-fos protein, a specific biomarker of neuronal activation (Herrera & Robertson, 1996), in the left PrL cortex increased significantly only in the SPIO+10 Hz MF group after 5 days of 10 Hz magnetic stimulation by the c-MSS (Figure 6A–C).

Secondly, injection of SPIO or Au without a magnetic field did not affect the behavioral tests in CUMS mice. Thus, control mice, CUMS mice, and CUMS mice treated with 10 Hz c-MSS for 5 days were used to measure depression markers. Here, BDNF, a consistent biomarker indicating severity of depressive symptoms and efficacy of anti-depressive therapies (Karege et al., 2005; Molendijk et al., 2014), was markedly decreased in the left PrL cortex of CUMS mice (Figure 6D) and significantly up-regulated after c-MSS treatment.

Finally, the serum levels of CORT and ACTH, indicators of HPA axis activity and biomarkers of depression and anti-depressive symptoms (Müller & Holsboer, 2006; Pariante & Lightman, 2008), respectively, became normalized in CUMS mice after c-MSS treatment (Figure 6E, F).

DISCUSSION

The principal findings of the present study include the following: (1) A novel c-MSS for brain stimulation with a mild magnetic field was established; (2) c-MSS treatment with a 100 mT/10 Hz magnetic field for 5 days (2×5 min sessions per day) markedly improved depressive-like behavior in CUMS mice, which was simultaneously indicated by changes in therapeutic biomarkers; and (3) Microinjected SPIO nanoparticles in the left PrL cortex remained stable for 11 days and were relatively safe and non-toxic both in cultured cells and brain tissue of mice. Taken together, these results suggest that the c-MSS, representing selective/targeted magnetic stimulation of the left PrL cortex, played an important role in reversing depressive symptoms in CUMS mice.

Here, for the first time, the novel c-MSS employed a mild magnetic field with microinjected SPIO nanoparticles to elevate local tissue magnetic susceptibility, thereby making the magnetic effect act upon deep brain structures and improve the precision of magnetic stimulation of a focused region in mice. Therefore, the c-MSS has overcome the technical bottleneck of rTMS, in which the magnetic effect is focused to activate the cortex, but the magnetic field covers a wide area. This new technique is particularly suitable for small animals.

SPIO (PSC@γ-Fe_2O_3) nanoparticles have been approved by the FDA for use as a nanodrug (Sun et al., 2019). The SPIO nanoparticles, whether utilized on primary cultured neuronal cells or injected into the left PrL cortex, were shown to be relatively safe and non-toxic. Importantly, the SPIO nanoparticles maintained stability within the PrL cortex for 11 days, longer than the experimental course of treatment (7 days). However, it should be noted that these results do not imply that SPIO nanoparticles are not metabolized in brain tissue in mice. Evidence from previous MRI tracing of SPIO nanoparticles in mouse brains suggests that SPIO nanoparticles initially reduce in number after two weeks, and then undergo a significant reduction after four weeks until they are barely visible at eight weeks (unpublished data). In summary, the present study provides evidence that SPIO nanoparticles are safe and stable for injection into brain tissue for short periods in mice.

We further demonstrated greater neuronal activity in mice after stimulation by the c-MSS, as indicated by increased expression of c-fos in the left PrL cortex. An important question is how c-MSS induces neuronal activity through magnetic stimulation. Firstly, evaluation of magnetic heating in the phantom indicated that the SPIO nanoparticles caused a negligible rise in temperature, important for the safety of magnetic stimulation as there is concern about brain heating in clinical practice. Secondly, magnetic vibration in the phantom indicated just the slightest vibration. Based on the simulated results, the physical effects of SPIO nanoparticles were highly localized. This means the increased energy

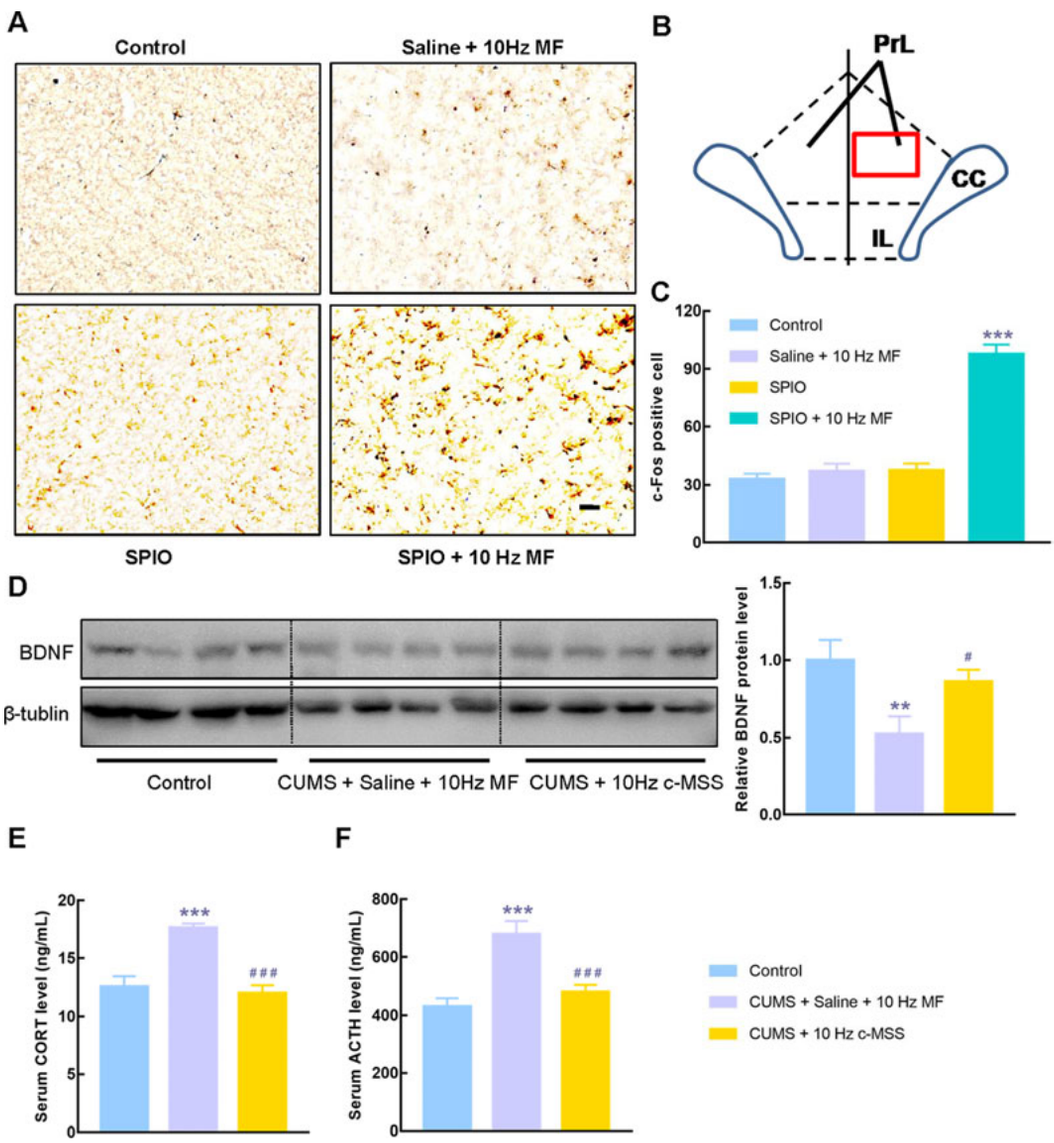

Figure 6 Comparison of biomarker levels for effective anti-depression in mice

A: Representative immunohistochemistry micrographs of c-fos expression in left PrL cortex after c-MSS treatment for 5 days in mice. B: Schematic displaying region of left PrL cortex. C: c-fos-positive cells in left PrL cortex. Scale bar: 50 μm. n=8 slices from eight mice in each group. Values represent mean±*SEM*. ***: P<0.001 vs. Control (one-way ANOVA followed by Bonferroni's multiple comparison *post hoc* test). D: BDNF protein levels in PrL whole tissue in various groups. E: Serum levels of CORT in various groups. F: Serum levels of ACTH in various groups. Data were calculated from eight mice for each group. Values are mean±*SEM*. **: P<0.01 vs. Control; ***: P<0.001 vs. Control. #: P<0.05 vs. CUMS+Saline+10 Hz MF; ###: P<0.001 vs. CUMS+Saline+10 Hz MF (one-way ANOVA followed by Bonferroni's multiple comparison *post hoc* test). PrL: Prelimbic; CUMS: Chronic unpredictable mild stress; BDNF: Brain-derived neurotrophic factor; CORT: Corticosterone; ACTH: Adrenocorticotropic hormone.

quickly dissipated with increasing distance. Thus, the effect of the c-MSS was localized around the SPIO nanoparticles without remote influences. However, enhanced induction of electrical voltage could be measured, which results from the high conductivity of PBS buffer in the phantom. As the physiological medium is also highly conductive, the enhancement of induction electric field may be an important physical mechanism. Recent study has also suggested that magnetic nanoparticles enhance performance of rTMS (Li et al., 2019).In the current study, we first adopted the CUMS mouse model to verify rapid antidepressant action by the c-MSS with the optimized strategy of 5 days of 10 Hz magnetic stimulation (100 mT, 5 min/session, two sessions daily). Compared with the controls, a 100 mT magnetic field alone did not cause an anti-depressive effect resulting from the low field intensity. Although the magnetic field was applied to

multiple cortices, the therapeutic effects were caused by the presence of the SPIO nanoparticles in which the PrL cortex was activated by mild stimulation. This point was established by the results of injection of Au nanoparticles and the expression of c-fos. Thus, it is possible to precisely stimulate a specific cortex using c-MSS.

Additionally, behavioral tests confirmed antidepressant action, with c-MSS significantly reversing abnormal levels of BDNF and HPA axis activity (CORT and ACTH) in CUMS mice, further confirming the effectiveness of this novel technique. As a biomarker of therapeutic effect, BDNF is consistently up-regulated after treatment with antidepressants, including drugs and physical therapy in both animal models and patients (Ghosal et al., 2018; Oh et al., 2019). Clinical evidence indicates that 10 Hz is the optimal frequency for treatment of MDD. In general, it takes 3–5 weeks to significantly improve patient symptoms (George & Post, 2011). Previous studies have shown that the most significant anti-depressive effects are observed after 10 days of 10 Hz TMS stimulation in small animals (Hesselberg et al., 2016). Here, with mild c-MSS precisely stimulating the PrL cortex, depressive-like behavior in CUMS mice improved significantly in just 5 days. A wide range of studies have examined the delivery of stimulation at different pulse frequencies during rTMS-mediated treatment of depression (Trevizol & Blumberger, 2019). As a result, both low-frequency (1 Hz, typically delivered to right DLPFC) (Berlim et al., 2013) and high-frequency (5–20 Hz, typically delivered to left DLPFC) (Berlim et al., 2014) rTMS have been found to be efficacious for the management of depression. Among the distinct frequencies, the now-standard 10 Hz rTMS for depression therapy has been widely accepted in clinical settings. Recent evidence suggests that active 5 Hz or 20 Hz rTMS may markedly improve clinical symptoms in depressed individuals when compared with sham rTMS (George et al., 2000; Luborzewski et al., 2007; Philip et al., 2015; Stubbeman et al., 2018; Su et al., 2005). However, the primary limitations of 5 Hz or 20 Hz rTMS include modest clinical sample sizes and uncertain clinical safety and treatment tolerability (Hadley et al., 2011; Loo et al., 2008; McGirr et al., 2016). In the present study, we found that depressive-like behaviors were markedly ameliorated in CUMS mice by stimulation with 10 Hz c-MSS for 5 days, but not 2 Hz or 5 Hz c-MSS. In light of the clinical effectiveness of 5 Hz or 20 Hz c-MSS in depression, we cannot exclude the possibility that 5 Hz treatment may produce an antidepressant effect over a longer period (more than 1 week, even 2 weeks), which deserves further study. Likewise, the effects of 20 Hz c-MSS on depressive symptoms in CUMS mice will be carried out in our future research. In addition, it will be interesting to measure the direct effects of 10 Hz stimulation on neuronal spikes, which may provide novel insights into the effectiveness of 10 Hz c-MSS in the treatment of depression.

In previous studies on small animals, magnetic fields such as in rTMS covered the entire hemisphere, and sometimes even the whole brain, which includes many cortices and deep nuclei. Activation of multiple cortices could result in counteracting effects so that therapeutic performance is insignificant. Our results demonstrate that this novel stimulation strategy is feasible and beneficial in mice, compared to traditional stimulation strategies. Our next goal is to realize the non-invasive administration of SPIO nanoparticles via veins into the cortex. This will boost the clinical translation of this technique.

Therefore, c-MSS could potentially expand the scope of magnetic stimulation applications. Firstly, SPIO nanodrugs are injectable, thereby greatly reducing the risk of implantation surgery. Secondly, the technology allows precise stimulation of practically any cortex using a mild magnetic field. Thus, we believe this strategy has considerable potential as a candidate system for improvement in neural regulation for exploration of brain activity mechanisms.

CONCLUSIONS

We demonstrated a novel c-MSS for magnetic brain stimulation in mice, in which the left PrL cortex was targeted, significantly improving treatment of depressive-like behavior in CUMS mice using a 10 Hz magnetic field for 2×5 min sessions per day for 5 days. The treatment also improved biomarkers of therapeutic effects. Importantly, the SPIO nanoparticles, a relative safe and non-toxic nano-drug, markedly enhanced local brain tissue susceptibility, possibly through neuronal activation of magneto-electric induction. In addition, the nano-drug remained stably localized after microinjection into the left PrL cortex of mice for 11 days. Therefore, we believe that the c-MSS improves the selective and precise regulation of neural circuits, thus allowing additional exploration of activated brain magnetic mechanisms. This method therefore has potential clinical value.

SUPPLEMENTARY DATA

Supplementary data to this article can be found online.

COMPETING INTERESTS

The authors declare that they have no competing interests.

AUTHORS' CONTRIBUTIONS

J.F.S. and Z.J.Z. designed the study, reviewed the data, and prepared the manuscript. Q.B.L. and Q.Y.Y., with help from M.Q.X. and W.W.C., performed the animal experiments and MRI tracings, prepared the figures, and drafted the manuscript. N.G. provided the magnetic iron oxide nanoparticles and valuable discussions about this project. J.F.S. fabricated the hydrogel phantom and constructed the pulse magnetic field. All authors read and approved the final version of the manuscript.

ACKNOWLEDGMENTS

Dr. Jiao Jiao from the Xinxiang Medical College and Prof. Hui

Xia from the Institute of Electric Engineering, Chinese Academy of Sciences, are greatly appreciated for help measuring the magneto-electric induction and magneto-vibration effects. Li-Hong Xu and Huan-Yi Zhu are appreciated for measurement of magnetic heating.

REFERENCES

Berlim MT, van den Eynde F, Jeff Daskalakis Z. 2013. Clinically meaningful efficacy and acceptability of low-frequency repetitive transcranial magnetic stimulation (rTMS) for treating primary major depression: a meta-analysis of randomized, double-blind and sham-controlled trials. *Neuropsychopharmacology*, **38**(4): 543−551.

Berlim MT, van den Eynde F, Tovar-Perdomo S, Daskalakis ZJ. 2014. Response, remission and drop-out rates following high-frequency repetitive transcranial magnetic stimulation (rTMS) for treating major depression: a systematic review and meta-analysis of randomized, double-blind and sham-controlled trials. *Psychological Medicine*, **44**(2): 225−239.

Bestmann S. 2008. The physiological basis of transcranial magnetic stimulation. *Trends in Cognitive Sciences*, **12**(3): 81−83.

Chen R, Romero G, Christiansen MG, Mohr A, Anikeeva P. 2015. Wireless magnetothermal deep brain stimulation. *Science*, **347**(6229): 1477−1480.

Diana M, Raij T, Melis M, Nummenmaa A, Leggio L, Bonci A. 2017. Rehabilitating the addicted brain with transcranial magnetic stimulation. *Nature Reviews Neuroscience*, **18**(11): 685−693.

Fang GX, Wang Y. 2018. Effects of rTMS on hippocampal endocannabinoids and depressive-like behaviors in adolescent rats. *Neurochemical Research*, **43**(9): 1756−1765.

GBD 2016 Disease and Injury Incidence and Prevalence Collaborators. 2017. Global, regional, and national incidence, prevalence, and years lived with disability for 328 diseases and injuries for 195 countries, 1990-2016: a systematic analysis for the Global Burden of Disease Study 2016. *The Lancet*, **390**(10100): 1211−1259.

George MS, Nahas Z, Molloy M, Speer AM, Oliver NC, Li XB, Arana GW, Risch SC, Ballenger JC. 2000. A controlled trial of daily left prefrontal cortex TMS for treating depression. *Biological Psychiatry*, **48**(10): 962−970.

George MS, Post RM. 2011. Daily left prefrontal repetitive transcranial magnetic stimulation for acute treatment of medication-resistant depression. *The American Journal of Psychiatry*, **168**(4): 356−364.

Ghosal S, Bang E, Yue WZ, Hare BD, Lepack AE, Girgenti MJ, Duman RS. 2018. Activity-dependent brain-derived neurotrophic factor release is required for the rapid antidepressant actions of scopolamine. *Biological Psychiatry*, **83**(1): 29−37.

Guadagnin V, Parazzini M, Fiocchi S, Liorni I, Ravazzani P. 2016. Deep transcranial magnetic stimulation: modeling of different coil configurations. *IEEE Transactions on Biomedical Engineering*, **63**(7): 1543−1550.

Guduru R, Liang P, Hong J, Rodzinski A, Hadjikhani A, Horstmyer J, Levister E, Khizroev S. 2015. Magnetoelectric 'spin' on stimulating the brain. *Nanomedicine*, **10**(13): 2051−2061.

Hadley D, Anderson BS, Borckardt JJ, Arana A, Li XB, Nahas Z, George MS. 2011. Safety, tolerability, and effectiveness of high doses of adjunctive daily left prefrontal repetitive transcranial magnetic stimulation for treatment-resistant depression in a clinical setting. *The Journal of ECT*, **27**(1): 18−25.

Hauer L, Sellner J, Brigo F, Trinka E, Sebastianelli L, Saltuari L, Versace V, Höller Y, Nardone R. 2019. Effects of repetitive transcranial magnetic stimulation over prefrontal cortex on attention in psychiatric disorders: a systematic review. *Journal of Clinical Medicine*, **8**(4): 416.

Herrera DG, Robertson HA. 1996. Activation of c-fos in the brain. *Progress in Neurobiology*, **50**(2-3): 83−107.

Hesselberg ML, Wegener G, Buchholtz PE. 2016. Antidepressant efficacy of high and low frequency transcranial magnetic stimulation in the FSL/FRL genetic rat model of depression. *Behavioural Brain Research*, **314**: 45−51.

Huang H, Delikanli S, Zeng H, Ferkey DM, Pralle A. 2010. Remote control of ion channels and neurons through magnetic-field heating of nanoparticles. *Nature Nanotechnology*, **5**(8): 602−606.

Karege F, Bondolfi G, Gervasoni N, Schwald M, Aubry JM, Bertschy G. 2005. Low brain-derived neurotrophic factor (BDNF) levels in serum of depressed patients probably results from lowered platelet BDNF release unrelated to platelet reactivity. *Biological Psychiatry*, **57**(9): 1068−1072.

Li K, Nejadnik H, Daldrup-Link HE. 2017. Next-generation superparamagnetic iron oxide nanoparticles for cancer theranostics. *Drug Discovery Today*, **22**(9): 1421−1429.

Li RR, Wang J, Yu XY, Xu PF, Zhang S, Xu JH, Bai YJ, Dai ZZ, Sun YX, Ye RD, Liu XF, Ruan G, Xu GL. 2019. Enhancing the effects of transcranial magnetic stimulation with intravenously injected magnetic nanoparticles. *Biomaterials Science*, **7**(6): 2297−2307.

Loo CK, McFarquhar TF, Mitchell PB. 2008. A review of the safety of repetitive transcranial magnetic stimulation as a clinical treatment for depression. *International Journal of Neuropsychopharmacology*, **11**(1): 131−147.

Luborzewski A, Schubert F, Seifert F, Danker-Hopfe H, Brakemeier EL, Schlattmann P, Anghelescu I, Colla M, Bajbouj M. 2007. Metabolic alterations in the dorsolateral prefrontal cortex after treatment with high-frequency repetitive transcranial magnetic stimulation in patients with unipolar major depression. *Journal of Psychiatric Research*, **41**(7): 606−615.

McGirr A, Karmani S, Arsappa R, Berlim MT, Thirthalli J, Muralidharan K, Yatham LN. 2016. Clinical efficacy and safety of repetitive transcranial magnetic stimulation in acute bipolar depression. *World Psychiatry*, **15**(1): 85−86.

Meng QL, Cherry M, Refai A, Du XM, Lu HB, Hong E, Yang YH, Choa FS. 2018. Development of focused transcranial magnetic stimulation for rodents by copper-array shields. *IEEE Transactions on Magnetics*, **54**(5): 9300504.

Molendijk ML, Spinhoven P, Polak M, Bus BAA, Penninx BWJH, Elzinga BM. 2014. Serum BDNF concentrations as peripheral manifestations of depression: evidence from a systematic review and meta-analyses on 179 associations (N=9484). *Molecular Psychiatry*, **19**(7): 791−800.

Müller MB, Holsboer F. 2006. Mice with mutations in the HPA-system as models for symptoms of depression. *Biological Psychiatry*, **59**(12): 1104−1115.

Oh H, Piantadosi SC, Rocco BR, Lewis DA, Watkins SC, Sibille E. 2019. The role of dendritic brain-derived neurotrophic factor transcripts on altered inhibitory circuitry in depression. *Biological Psychiatry*, **85**(6): 517−526.

Otte C, Gold SM, Penninx BW, Pariante CM, Etkin A, Fava M, Mohr DC, Schatzberg AF. 2016. Major depressive disorder. *Nature Reviews Disease Primers*, **2**: 16065.

Pariante CM, Lightman SL. 2008. The HPA axis in major depression: classical theories and new developments. *Trends in Neurosciences*, **31**(9):

464−468.

Pascual-Leone A, Rubio B, Pallardó F, Catalá MD. 1996. Rapid-rate transcranial magnetic stimulation of left dorsolateral prefrontal cortex in drug-resistant depression. *The Lancet*, **348**(9022): 233−237.

Philip NS, Carpenter SL, Ridout SJ, Sanchez G, Albright SE, Tyrka AR, Price LH, Carpenter LL. 2015. 5 Hz Repetitive transcranial magnetic stimulation to left prefrontal cortex for major depression. *Journal of Affective Disorders*, **186**: 13−17.

Polanía R, Nitsche MA, Ruff CC. 2018. Studying and modifying brain function with non-invasive brain stimulation. *Nature Neuroscience*, **21**(2): 174−187.

Roet M, Hescham SA, Jahanshahi A, Rutten BPF, Anikeeva PO, Temel Y. 2019. Progress in neuromodulation of the brain: a role for magnetic nanoparticles?. *Progress in Neurobiology*, **177**: 1−14.

Salvador R, Miranda PC. 2009. Transcranial magnetic stimulation of small animals: a modeling study of the influence of coil geometry, size and orientation. In: Proceedings of 2009 Annual International Conference of the IEEE Engineering in Medicine and Biology Society. Minneapolis, MN, USA: IEEE, 2009: 674–677.

Stubbeman WF, Zarrabi B, Bastea S, Ragland V, Khairkhah R. 2018. Bilateral neuronavigated 20Hz theta burst TMS for treatment refractory depression: an open label study. *Brain Stimulation*, **11**(4): 953−955.

Su TP, Huang CC, Wei IH. 2005. Add-on rTMS for medication-resistant depression: a randomized, double-blind, sham-controlled trial in Chinese patients. *The Journal of Clinicalpsychiatry*, **66**(7): 930−937.

Sun JF, Zhang Y, Yang F, Ma M, Xiong F, Gu N. 2019. Research and development of medical magnetic nanomaterials. *Science Bulletin*, **64**(8): 842−853.

Sun P, Wang FR, Wang L, Zhang Y, Yamamoto R, Sugai T, Zhang Q, Wang ZD, Kato N. 2011. Increase in cortical pyramidal cell excitability accompanies depression-like behavior in mice: a transcranial magnetic stimulation study. *The Journal of Neuroscience*, **31**(45): 16464−16472.

Tang AD, Lowe AS, Garrett AR, Woodward R, Bennett W, Canty AJ, Garry MI, Hinder MR, Summers JJ, Gersner R, Rotenberg A, Thickbroom G, Walton J, Rodger J. 2016. Construction and evaluation of rodent-specific rTMS coils. *Frontiers in Neural Circuits*, **10**: 47.

Tarapore PE, Picht T, Bulubas L, Shin Y, Kulchytska N, Meyer B, Berger MS, Nagarajan SS, Krieg SM. 2016. Safety and tolerability of navigated TMS for preoperative mapping in neurosurgical patients. *Clinical Neurophysiology*, **127**(3): 1895−1900.

Trevizol AP, Blumberger DM. 2019. An update on repetitive transcranial magnetic stimulation for the treatment of major depressive disorder. *Clinical Pharmacology and Therapeutics*, **106**(4): 747−762.

Vertes RP. 2006. Interactions among the medial prefrontal cortex, hippocampus and midline thalamus in emotional and cognitive processing in the rat. *Neuroscience*, **142**(1): 1−20.

Yue K, Guduru R, Hong J, Liang P, Nair M, Khizroev S. 2012. Magneto-electric nano-particles for non-invasive brain stimulation. *PLoS One*, **7**(9): e44040.